

Pinch Oscillations in Electron-Hole Plasmas. I. Theory

W. S. CHEN* AND B. ANCKER-JOHNSON

*Boeing Scientific Research Laboratories, Seattle, Washington 98124 and
University of Washington,† Seattle, Washington 98105*

(Received 2 June 1970)

The Drummond–Ancker-Johnson magnetothermal pinch theory which describes the oscillations in electron-hole plasmas is extended. The theory is based on only two fundamental equations, the power-balance equation in the inner region of the pinch and the particle-conservation equation in the outer region of the pinch. By perturbing the two fundamental equations from their quasiequilibrium states, a dispersion relation is obtained which predicts oscillations in the electric field strength, provided specific conditions are satisfied. When the experimental dependencies of the frequency on current and time are incorporated into the equations, a theoretically determined inner current I_i and outer temperature T_0 are obtained. These values of I_i and T_0 are uniquely defined, and their behavior is consistent with the observed dependence of the oscillation amplitude on current and time. These results are also consistent with the known thermal conductance of InSb. The theory predicts that the pinch radius expands somewhat as time progresses. Although the theory invokes several simplifying assumptions, it agrees well with the observed properties of the pinch oscillations. On the basis of this agreement, it is concluded that the theory is basically correct.

I. INTRODUCTION

It is a well-known fact that a strong current can produce pinching of nonequilibrium electron-hole plasmas in InSb.¹ Reports on the first experiments in pinching of impact ionized² plasmas and injected plasmas³ in InSb included observations of small-amplitude oscillations in the voltage. Oscillations related to pinching have also been observed in the presence of applied transverse^{4,5} and longitudinal⁶⁻⁸ magnetic fields. Much larger, growing oscillations in *p*-InSb have been reported^{1,9} when the plasma is dissipating power in the range from 0.4 to ~ 2 kW/cm.

Several theories describe the response of nonequilibrium electrons and holes when compressed by a self-magnetic field. Glicksman¹⁰ produced a pinch theory under the assumption that the electron-hole gas in the pinch is compressed adiabatically. This assumption implies that the lattice thermal conductivity is zero; hence the theory is limited in validity to small currents and short-duration plasmas. Marechal¹¹ has presented a purely magnetic pinch theory which does not employ adequate restoring forces. Thus the predicted pinch radius is too small. Schmidt¹² assumes that the compression of the electron-hole gas in the pinch should occur isothermally due to the strong electron-phonon coupling. Hence, his results apply only to the early period of the pinch when the lattice is still cold. Paranjape,¹³ by taking into account the nonlinear recombination, successfully explains the resistivity change accompanying pinching. None of these theories predict the oscillatory phenomena.

Recently, Igitkhanov¹⁴ obtained a dispersion equation describing the pinch stability criterion. He generated this equation by perturbing the equilibrium pinch condition he derived from the two-fluid hydrodynamic model. His results predict a weak instability in the

long-wavelength limit. Since his results do not give an explicit dependence on the measurable quantities, no comparison between his theory and experiment is possible. Furthermore, he implicitly assumes adiabatic compression of the electron-hole plasma during pinch. Thus, Igitkhanov's theory is subject to the same limitations as Glicksman's.¹⁰

Distinctive to the Drummond–Ancker-Johnson (DAJ) theory,¹⁵ which also predicts voltage oscillations, is the assumption that the plasma is in good thermal contact with the lattice; hence DAJ's is a magnetothermal pinch effect. The two fundamental equations of DAJ are those for the conservation of carriers and energy in which the temperature-dependent mobilities and plasma densities are used. This theory accounts for thermal pinch,¹⁶ which occurs at power inputs $\gtrsim 2.9$ kW/cm, and demonstrates that oscillating voltages should occur at intermediate power-input levels, below those producing thermal pinching and above those producing simple magnetic pinching. The agreement with experiment is quantitative for thermal pinch. It is only qualitative for magnetothermal pinch since only qualitative solutions were obtained by an analog computer.

In Sec. II is an extension of the DAJ theory.¹⁵ Again, it is assumed that the plasma is in good thermal contact with the lattice. Furthermore, a two-region model of the pinch, a hot inner region and a cooler outer region, is again assumed. Results of the extended theory show under what conditions growing oscillations exist, thus enabling a detailed comparison with experiment.

In Sec. III the solutions, obtained by digital computer, are compared with measurements. Good quantitative agreement is found.

In the Conclusions the limitations of the theory are discussed. It is concluded that the magnetothermal interpretation of the pinch oscillations is correct.

II. THEORY

One result of the DAJ theory¹⁵ shows that the electric field strength has a nonsinusoidal oscillatory character at moderate power input ($0.4 < p < 2$ kW/cm) into the plasma, in agreement with the observations. In order to make a quantitative comparison between the theory and the experimental results, expressions explicitly specifying the dependencies of the oscillations are required.

In this analysis, a two-region model of the pinch is retained:

(1) *Inner region:* The plasma initially pinches down to a small, hot, and stable channel with temperature T_i , density n_i , and radius r .

(2) *Outer region:* The temperature T_0 in this region will also rise above the ambient temperature, because of thermal flux from the inner region. The number of plasma particles per unit length in the outer region, N_0 , will increase because of the effective kinetic pressure difference between the inner and outer region. The outer region forms a cylinder around the inner hot channel whose thickness is of the same order as r . Both of these dimensions are much smaller than the sample radius.

According to the DAJ theory,¹⁵ the temperature inside the hot channel, after the initial sharp rise, changes very little with respect to time. A nearly constant T_i means an essentially steady-state condition exists, so that the power input into the channel must equal the power conduction away from the channel:

$$I_i E = -2\pi r (\mathcal{L}/T_i) (\partial T_i / \partial r). \quad (1)$$

I_i is the current carried by the plasma inside the channel and \mathcal{L}/T is the thermal conductivity.¹⁷ Since the hole mobility is much less than the electron mobility in InSb, the very small current contributed by holes is neglected. Therefore,

$$I_i = \pi r^2 |e| n_i \mu_e E, \quad (2)$$

where μ_e is the electron mobility, n_i is density of carriers inside the channel, and E is the electric field strength. If the power balance condition, Eq. (1), is disturbed, the temperature T_i will increase at a rate given by

$$\partial T_i / \partial t = (1/\pi r^2 DC) [I_i E + 2\pi r (\mathcal{L}/T_i) (\partial T_i / \partial r)], \quad (3)$$

where D is the density of InSb crystal and C is its specific heat.

The spatial dependence of the temperature leads to the following form of the continuity equation: The particle conservation equation is $\partial n / \partial t = -\nabla \cdot n \mathbf{v}$, where $\mathbf{v} = \mu \mathbf{F} / |e|$ and

$$\mathbf{F} = -(2n)^{-1} [\nabla 2nkT + \mu^0 \mathbf{J} \times \mathbf{H}].$$

The last term represents the Lorentz force caused by the

self-magnetic field, and the factor 2 takes into account the presence of both electrons and holes. Hence the continuity equation has this form:

$$\partial n / \partial t = r^{-1} \partial / \partial r \{ (r\mu / |e|) [\partial / \partial r (nkT) + \frac{1}{2} \mu^0 (\mathbf{J} \times \mathbf{H})] \}. \quad (4)$$

To obtain the specific form of this equation, first the net pressure gradient directed outward from the hot channel is taken into account. It is

$$- [k (\partial n_i T_i / \partial r) + \frac{1}{2} \mu^0 J_i(r) H(r)], \quad (5a)$$

where k is the Boltzmann constant, μ^0 is the permeability and $J_i(r)$, $H(r)$ are the current density inside the hot channel and the self-magnetic field around this channel at r . Secondly, the pressure gradient at r caused by the plasma outside the channel pushing the particles inward is

$$k (\partial n_0 T_0 / \partial r), \quad (5b)$$

where n_0 is the plasma density in the outer region. Therefore, the ambipolar diffusion driven by the net pressure gradient increases the number of the plasma particles per unit length in the outer region at a rate given by

$$\partial N_0 / \partial t = - (2\pi r \mu_A / |e|) \times [k (\partial n_i T_i / \partial r) + \frac{1}{2} \mu^0 J_i(r) H(r) + k (\partial n_0 T_0 / \partial r)], \quad (6)$$

where μ_A is the ambipolar mobility in the outer region. This equation is obtained by integrating Eq. (4) over the cross-sectional area $r dr d\theta$.

Since the greatest rise in temperature will occur on the sample axis¹⁵ causing thermal ionization there, the density of carriers inside the channel becomes¹⁸

$$n_i = A T_i^{+3/2} Y, \quad (7)$$

where $Y = \exp[-\epsilon / (2kT_i)]$, A is a constant depending on the effective masses of the carriers, and ϵ is the band-gap energy. The electron mobility also depends on temperature. For temperatures exceeding 100 K it can be expressed¹⁹ as

$$\mu_e = \mu_0 T^{-x}, \quad (8)$$

where $x \approx 1.6$. For simplicity, the 1.6-power law is approximated by a $\frac{3}{2}$ -power law. Since the electron mobility far exceeds the hole mobility, the ambipolar mobility can be approximated by²⁰

$$\mu_A \approx (2m/M) \mu_e = (2m/M) \mu_0 T^{-3/2}, \quad (9)$$

where m/M is the electron-hole mass ratio.

Substituting (7) and (8) into (2) yields

$$I_i = \pi r^2 |e| A \mu_0 Y E \quad (10)$$

and hence,

$$H(r) = I_i / 2\pi r = r^2 |e| A \mu_0 Y E / 2r. \quad (11)$$

Also, the differentiation of nT with respect to r in (6)

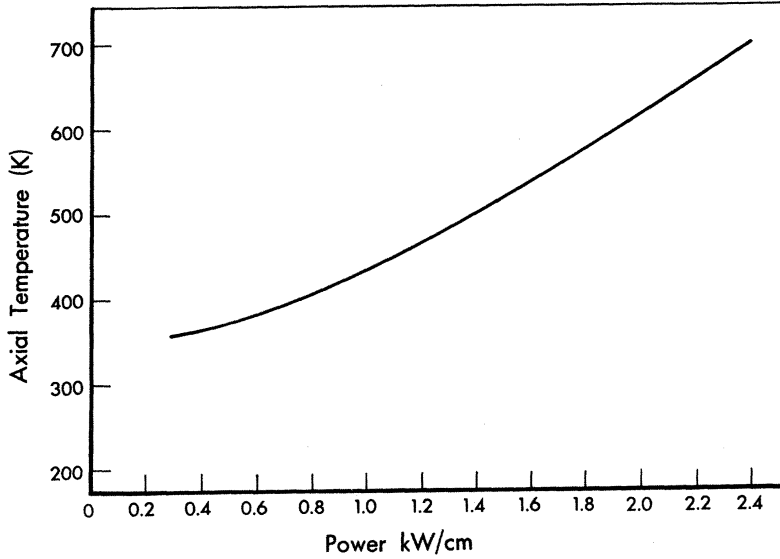


FIG. 1. Temperature on the axis of the pinch as a function of power dissipated by the pinch for an ambient of 77 K (Ref. 12).

may be approximated by

$$\partial n_i T_i / \partial r \approx -n_i T_i / r = -A T_i^{5/2} Y / r \quad (12)$$

and

$$\partial n_0 T_0 / \partial r \approx n_0 T_0 / r \approx N_0 T_0 / \pi r^3.$$

By using (9)–(12), the particle-conservation equations can be rewritten as

$$\begin{aligned} \partial N_0 / \partial t = & -(4\pi r m k \mu_0 T_0^{-3/2} / M | e |) \\ & \times [-A T_i^{5/2} Y / r + N_0 T_0 / \pi r^3] \\ & - (\pi r^2 m / M) (\mu^0 \mu_0^3 A^2 | e | Y^2 / T_i^{3/2}) E^2. \end{aligned} \quad (13)$$

The total current consists of three terms since the sample has three parts: an inner and outer pinch channel and all the rest of the sample. If the total current I_T is kept constant, the electric field strength becomes

$$E = \frac{I_T}{\pi r^2 | e | A \mu_0 Y + N_0 | e | \mu_0 T_0^{-3/2} + 1/R}, \quad (14)$$

where R is the Ohmic resistance per unit length of the sample.

If the nearly steady-state condition is perturbed, the temperature derivative in the inner region will change at a rate given approximately by

$$\delta \dot{T}_i = (\partial \dot{T}_i / \partial T_i) \delta T_i + (\partial \dot{T}_i / \partial N_0) \delta N_0, \quad (15)$$

where, by using (2), (3), and (14),

$$\begin{aligned} \partial \dot{T}_i / \partial T_i \equiv \alpha = & (1/\pi r^2 DC) (\partial / \partial T_i) \\ & \times [I_i E + 2\pi r (\mathcal{L}/T_i) (\partial T_i / \partial r)] \\ \approx & (1/\pi r^2 DC) (\epsilon/2kT_i^2) I_i E (1 - 2I_i/I_T) \end{aligned} \quad (16)$$

and

$$\begin{aligned} \partial \dot{T}_i / \partial N_0 \equiv \beta = & (1/\pi r^2 DC) (\partial / \partial N_0) \\ & \times [I_i E + 2\pi r (\mathcal{L}/T_i) (\partial T_i / \partial r)] \\ \approx & -(2I_i E^2 / \pi r^2 DC) (| e | / I_T) \mu_0 T_0^{-3/2}. \end{aligned} \quad (17)$$

The variation of $(1/T_i) \partial T_i / \partial r$ with temperature is neglected in these approximations since $\partial T_i / \partial r$ and T_i probably change proportionately to each other. It is also assumed that the radius r of the hot channel varies slowly with temperature.

Since the perturbation changes the temperature inside the channel, the time variation of the number of particles outside the channel will change accordingly, at a rate given by

$$\delta \dot{N}_0 = (\partial \dot{N}_0 / \partial T_i) \delta T_i + (\partial \dot{N}_0 / \partial N_0) \delta N_0, \quad (18)$$

where

$$\begin{aligned} \partial \dot{N}_0 / \partial T_i \equiv \gamma = & (4\pi r m k \mu_0 A Y / M | e |) (T_i / T_0)^{3/2} (\frac{3}{2} + \epsilon/2kT_i) \\ & + (2m/M) \mu^0 \mu_0 (I_i^2 / \pi r^2 | e |) T_i^{-5/2} [\frac{3}{2} + (\epsilon/kT_i) (I_i/I_T - 1)] \end{aligned} \quad (19)$$

and

$$\begin{aligned} \partial \dot{N}_0 / \partial N_0 \equiv \eta = & -(4\pi r m k \mu_0 / M | e |) (T_0^{-1/2} / \pi r^2) \\ & + (2m \mu^0 \mu_0^2 / M \pi r^2 T_i^{3/2} T_0^{3/2}) (I_i^2 E / I_T). \end{aligned}$$

If the perturbed quantities δT_i and δN_0 in Eqs. (15) and (18) have a time dependence which may be expressed as $\exp(pt)$, then

$$(p - \alpha) \delta T_i - \beta \delta N_0 = 0$$

and

$$-\gamma \delta T_i + (p - \eta) \delta N_0 = 0. \quad (20)$$

If there are nontrivial solutions, the determinant of the

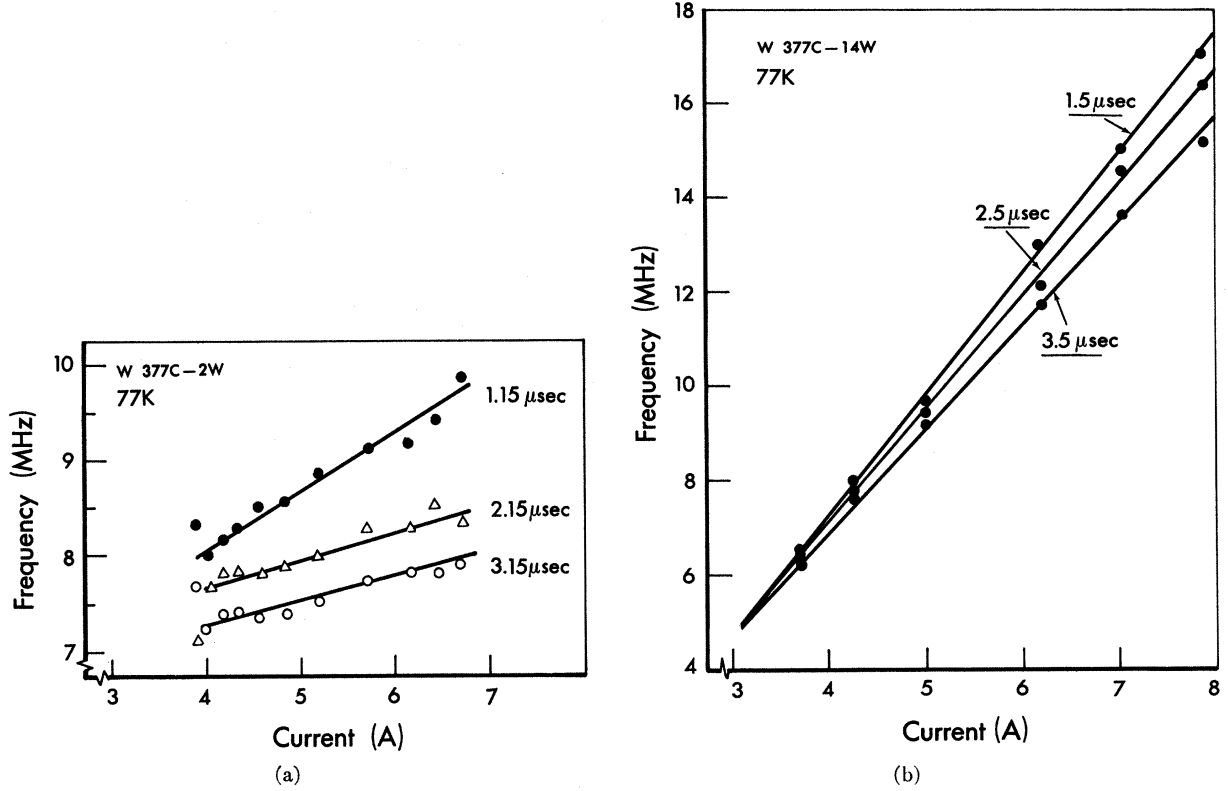


FIG. 2. (a) Measured frequency as a function of total current with time after the application of a voltage step as the parameter. For sample *W 377C-2W*. (b) Measured frequency as a function of total current with time after the application of a voltage step as the parameter. For sample *W 377C-14W*.

coefficients in (20) is zero:

$$\begin{vmatrix} p-\alpha & -\beta \\ -\gamma & p-\eta \end{vmatrix} = 0,$$

so

$$p = \frac{1}{2} \{ \alpha + \eta + [(\alpha - \eta)^2 + 4\beta\gamma]^{1/2} \}. \quad (21)$$

Therefore, the perturbations will grow in time with a temporal growth rate

$$\Gamma = \frac{1}{2} (\alpha + \eta) \geq 0. \quad (22)$$

Furthermore, the oscillation frequency of the perturbations is given by

$$f = (1/4\pi) \{ -[(\alpha - \eta)^2 + 4\beta\gamma] \}^{1/2}, \quad (23)$$

provided

$$(\alpha - \eta)^2 + 4\beta\gamma < 0.$$

The oscillatory nature of T_i and N_0 dictates that the electric field strength also oscillates, Eq. (14).

In order to make Γ and f easier to compute, they are expressed as follows by using (16)–(19) and (10):

$$\begin{aligned} 2\Gamma = & (A |e| \mu_0 Y E / I_i) [(1/DC) (\epsilon I_i E / 2kT_i^2) \\ & \times (1 - 2I_i / I_T) - (4\pi m k \mu_0 / M |e|) T_0^{-1/2} \\ & + (2m\mu^0 \mu_0^2 / M T_i^{3/2} T_0^{3/2}) (I_i^2 E / I_T)] \quad (24) \end{aligned}$$

and

$$\begin{aligned} 4\beta\gamma = & -(8 |e|^2 A \mu_0^2 Y^2 E^3 / DC I_T T_0^{3/2}) \\ & \times \{ (4\pi m k \mu_0 A / M |e|) (T_i / T_0)^{3/2} (\frac{3}{2} + \epsilon / 2kT_i) \\ & + (m/M) (\mu^0 A \mu_0^2 I_i E / T_i^{5/2}) [\frac{3}{2} + (\epsilon/kT_i) (I_i / I_T - 1)] \}. \quad (25) \end{aligned}$$

The constants appropriate to InSb are

$$\mu_0 = 3.7 \times 10^4 \text{ m}^2 \text{ K}^{3/2} / \text{V sec},^{21}$$

$$\epsilon = 0.225 \text{ eV},^{22}$$

$$D = 5.8 \times 10^3 \text{ kg/m}^3,^{23}$$

$$\mathcal{L} = 7 \times 10^3 \text{ J/sec m},^{17}$$

$$A = 4.2 \times 10^{20} \text{ K}^{-3/2} / \text{m}^3,^{18}$$

$$C = 100 \text{ J/kg K},^{24}$$

$$M/m \approx 30.^{25}$$

Since in the experiments (see following paper, Paper II) $E \approx 10^4 \text{ V/m}$, $T_0 \geq 77 \text{ K}$, and 77 K (ambient temperature) $< T_i < 800 \text{ K}$ (melting point), the first term in (24), a term contributed by α , is neglected compared

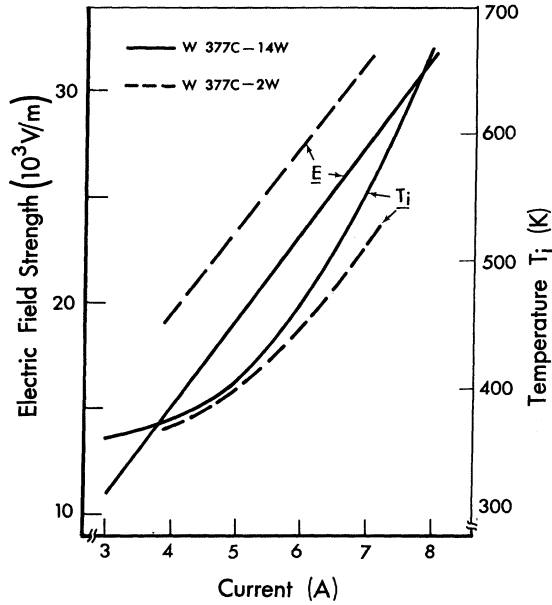


FIG. 3. Measured average electric field strength, and the temperature in the inner hot channel estimated from Fig. 1, as a function of total current for the two samples.

with the rest of the terms. Hence

$$2\Gamma \approx \eta = 2.86 \times 10^8 (YE/I_i T_i^{3/2} T_0^{3/2}) \times [EI_i^2/I_T - 1.16 \times 10^{-2} T_i^{3/2} T_0] \quad (26)$$

and

$$-4\beta\gamma = 1.14 \times 10^8 (Y^2 E^3 / I_T T_0^{3/2}) \times \left\{ (T_i/T_0)^{3/2} \left(\frac{3}{2} + \epsilon/2kT_i \right) + 43(I_i E / T_i^{5/2}) \left[\frac{3}{2} + (\epsilon/kT_i)(I_i/I_T - 1) \right] \right\}. \quad (27)$$

Consequently, the frequency can be rewritten as

$$f = (1/4\pi) [-(\eta^2 + 4\beta\gamma)]^{1/2}. \quad (28)$$

III. DISCUSSION

In order to compare the theoretical results with the experimental data, I_i , T_i , and T_0 must be determined. The temperature T_i inside the hot channel can be estimated from the axial temperature as a function of power input to the plasma, Fig. 1, obtained from the thermal pinch theory.¹⁵ The values of I_i and T_0 are very difficult to determine since they depend not only on I_T and E , but also on time. Therefore, the experimental data on frequency as a function of I_T are incorporated into the equations and the resulting values of I_i and T_0 are checked in several ways for consistency.

Figure 2 shows the dependency of the measured (see Paper II) frequencies on total current with time after the beginning of the pulse as a parameter, for two different samples. The onset of the oscillations occurs for sample No. 2, Fig. 2(a), at $I_T = 3.9$ A and the cutoff

at $I \approx 6.9$ A. For sample No. 14, Fig. 2(b), the onset is at $I_T = 3$ A and the cutoff at $I \approx 8$ A. The temperatures of the hot inner regions, estimated from Fig. 1, and the measured average electric field strengths are plotted in Fig. 3 as a function of the total current for these two samples.

A computer program determines the T_0 and I_i by fitting Eqs. (26)–(28) to the data in Figs. 2 and 3. During the computer calculations, for given values of I_T , E , and T_i , first the calculated frequency is plotted as a function of T_0 with the growth rate set equal to zero, as shown by the upper curve in Fig. 4. The dashed line in Fig. 4 shows the value of the measured frequency at the given I_T and E . For $\Gamma = 0$, one boundary solution of T_0 exists and the corresponding I_i is thus determined. Secondly, the calculated frequency is plotted with I_i as a parameter, the three lower curves in Fig. 4. When I_i equals a certain value, say, I_{iM} , a unique solution of T_0 is found; this is the tangency condition in Fig. 4. It defines a second boundary condition on the determinations of T_0 and Γ because no solution for T_0 exists when $I_i > I_{iM}$.

The growth rate $\Gamma (= \eta)$ is set equal to zero for the first fit, since this condition defines the boundary between stability and instability, and thus the onset

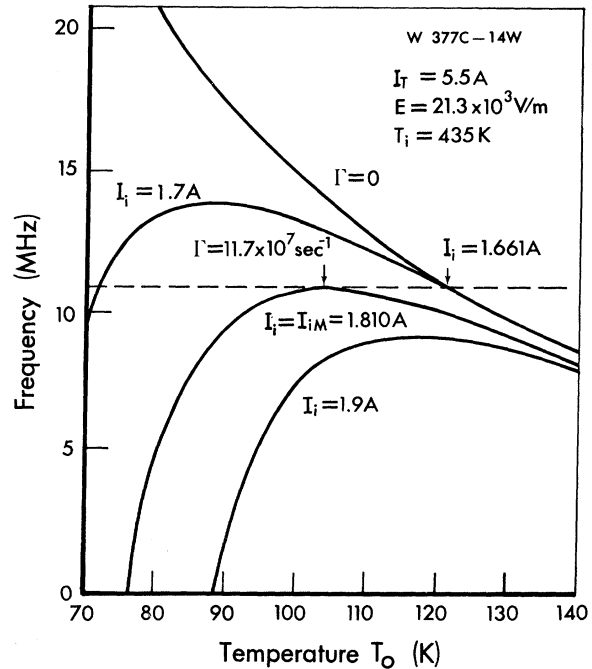


FIG. 4. Computer fitting procedure. At the growth rate $\Gamma = 0$, the frequency is calculated as a function of T_0 . The intersection of the frequency curve for $\Gamma = 0$ with the measured frequency (dashed line) is used to determine one boundary of T_0 and I_i . A second boundary is determined by the tangency condition in the plot of the calculated frequency with I_i as the parameter; at this boundary $2\Gamma = 11.7 \times 10^7 \text{ sec}^{-1}$. Note added in proof. The factor 2 is missing in the figure.

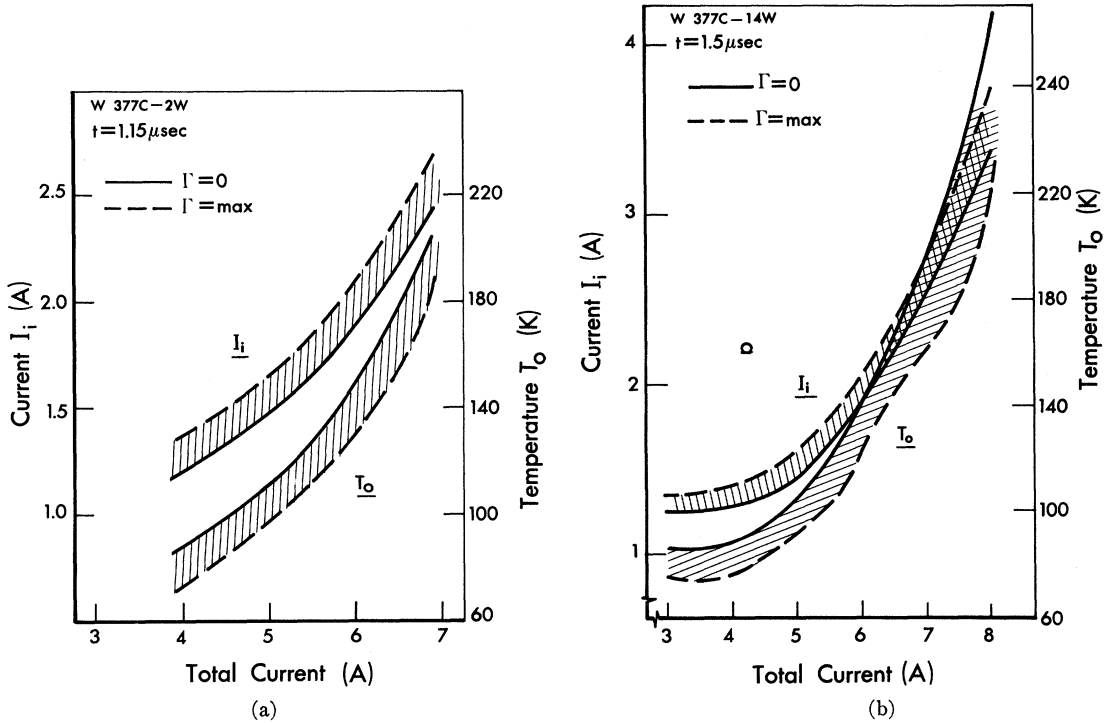


FIG. 5. (a) T_0 and I_i determined by fitting the theory and experiment as a function of total current. The solid lines are the values obtained by using the $\Gamma=0$ solution. The dashed lines are the solutions corresponding to the maximum allowed Γ . The two boundaries (solid and dashed lines) define values of T_0 and I_i which yield compatibility between the theory and the measured frequency. For sample *W 377C-2W*. (b) T_0 and I_i determined by fitting the theory and experiment as a function of total current. The solid lines are the values obtained by using the $\Gamma=0$ solution. The dashed lines are the solutions corresponding to the maximum allowed Γ . The two boundaries (solid and dashed lines) define values of T_0 and I_i which yield compatibility between the theory and the measured frequency. For sample *W 377C-14W*.

conditions for oscillation. The results are shown as solid lines in Fig. 5 for the two samples. The current carried by the hot inner region increases with total current because plasma is generated by thermal ionization as the temperature T_i increases. The computer solution also shows that the inner current I_i is $\sim \frac{1}{3}I_T$, the total current, which means the outer region of the pinch carries the most current, and thus the pinch is somewhat hollow. This result, which is not intuitively expected, is in agreement with the DAJ theory.¹⁵ The temperature rise in the outer region, T_0 , is caused by the heat conduction from the inner region. Since at a given time, T_i increases with I_T , Fig. 3, T_0 should also. This expectation is borne out by the results in Fig. 5.

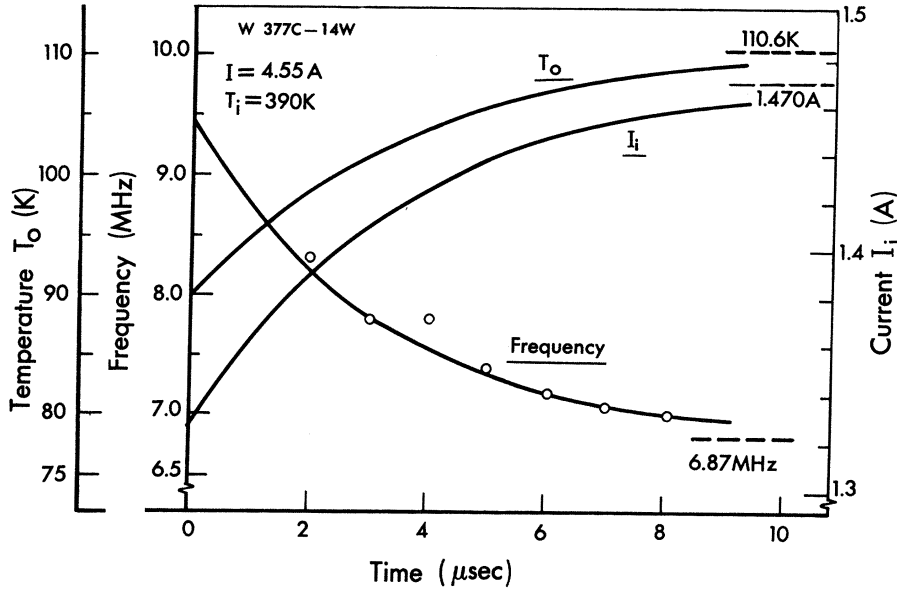
The upper limit of I_i and the lower limit of T_0 are determined by the condition $I_i = I_{iM}$, dashed lines in Fig. 5. This condition produces the same dependency of I_i and T_0 on the total current as did the zero-growth-rate condition; in fact, the new values of I_i and T_0 are very close to those determined by the condition $\Gamma=0$.

The condition $I_i = I_{iM}$ results in an exceedingly high growth rate, $\Gamma \approx 10^8 \text{ sec}^{-1}$ as shown in Fig. 4. Such a

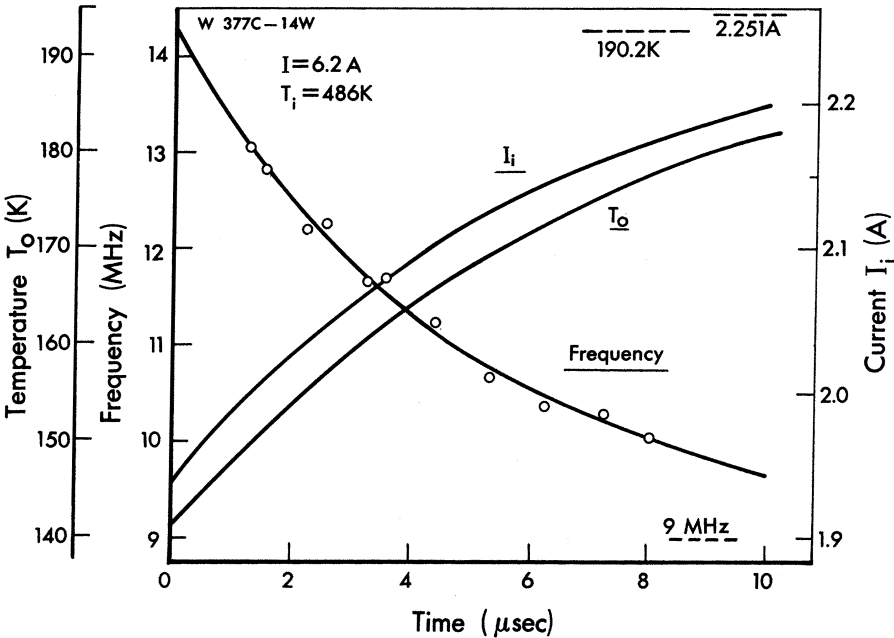
high growth rate is not compatible with the experimental results on oscillation amplitude as a function of current, as shown in Paper II, because the measured oscillation amplitude is proportional to the value of $\exp(\Gamma t)$. Thus, the correct values of I_i and T_0 must be very close to those values for which $\Gamma=0$. Hence it can be concluded that the current I_i in the inner region and temperature T_0 in the outer region are uniquely defined by the $\Gamma=0$ solutions.

So far in the comparison between theory and experiment, only the dependency of the parameters on total current has been considered. Another variable is time. The frequency as a function of time (up to $10 \mu\text{sec}$) at two current levels is shown in Fig. 6. It decreases exponentially. By fitting the theory to this frequency dependence, T_0 and I_i as functions of time are obtained. The temperature T_0 increases exponentially with time, a result that is consistent with the principle of heat conduction.²⁶

In order to test the self-consistency of the theory, the thermal conductivity (k_0) variation with temperature resulting from the fit between theory and experiment, is compared with the $k_0(T)$ data in the literature.



(a)



(b)

FIG. 6. (a) Measured frequency and computer-calculated T_0 and I_i as a function of time after the beginning of the pulse for $W 377C-14W$. This figure corresponds to a total current $I = 4.55 \text{ A}$. The short dashed lines at the end of each curve are the asymptotic values. (b) Measured frequency and computer-calculated T_0 and I_i as a function of time after the beginning of the pulse for $W 377C-14W$. This figure corresponds to a total current $I = 6.2 \text{ A}$. The short dashed lines at the end of each curve are the asymptotic values.

The $k_0(T)$ dependence emerging from the fit is found as follows: First it is noted from the thermal conduction equation

$$\partial T / \partial t = (k_0 / CD) \nabla^2 T \quad (29)$$

that temperature changes with time according to $\exp[(-k_0 / CD)\gamma^2 t]$, where γ is the separation constant. Thus, k_0 is inversely proportional to the time constant

of $T_0(t)$. Second, several $T_0(t)$ curves for one sample at different current levels are obtained by the fitting procedure described above. Three such curves are shown in Fig. 7 along with the temperature at steady state (dashed lines at left). The difference between the latter and $T_0(t)$ is found to be exponential in time for a given current level. Third, from the resulting time constants $k_0(T)$ is deduced and plotted, normalized to

its value at the median temperature, along with the known¹⁷ \mathcal{E}/T data, Fig. 8. The extent of agreement between the temperature dependence of thermal conductivity resulting from the fit between theory and experiment and the measured relationship produces more confidence in the correctness of this theory.

The current I_i for both cases, Fig. 6, increases with time. This increase is due to the expansion of the hot channel with time. The temperature T_0 at a low current level approaches a steady state faster than it does at a high current level, as the comparisons of the T_0 curves in Fig. 6 illustrate. This is a result of higher thermal conductivities occurring at lower temperatures.

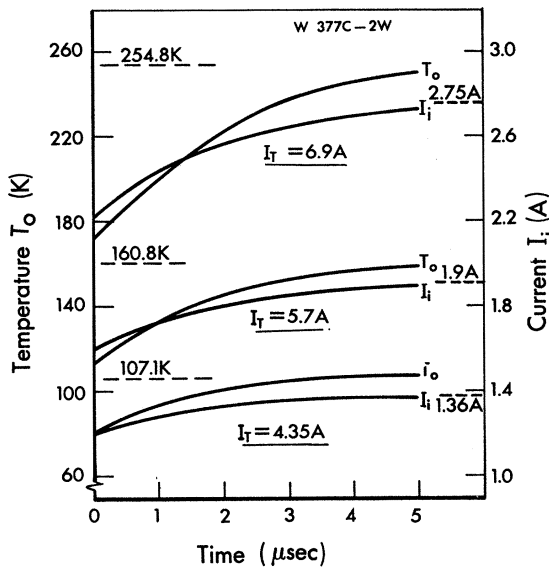


FIG. 7. The calculated T_0 and I_i as functions of time obtained by fitting the theory to the measured frequency for the sample W 377C-2W at three different current levels. The dashed lines are the asymptotic values.

By using Eq. (10) the radius, normalized to its value at $t=0$, is calculated as a function of time. As shown in Fig. 9 the radius for the two selected cases increases with time until a steady state is reached, consistent with the predicted hollow pinch.¹⁵ The calculated steady-state radius for the higher current level is 1.2×10^{-3} cm and for the lower current level, 1.6×10^{-3} cm, which agrees very well with the radius of the melted channel (2.8×10^{-3} cm) observed after thermal pinch.¹⁶

IV. CONCLUSIONS

The theory, since it assumes a two-region model for the pinch and a temperature-dependent mobility, is based on only two fundamental equations, the power-balance equation (1), in the inner region and the

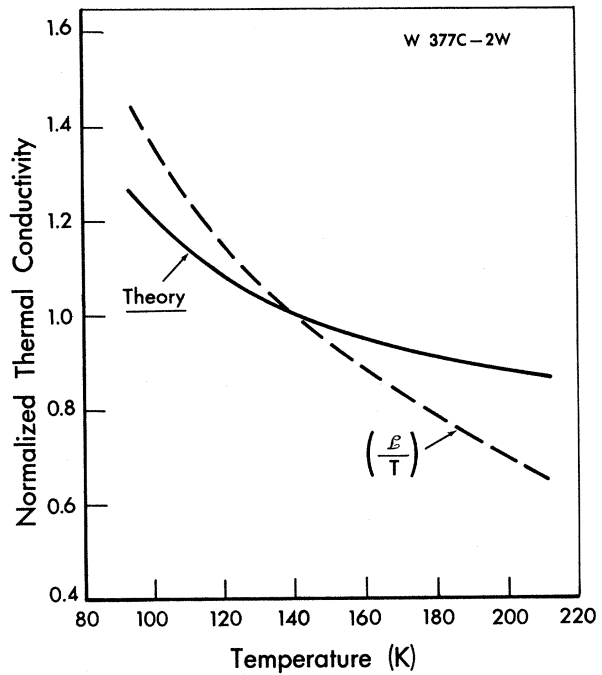


FIG. 8. Thermal conductivity deduced from its inverse proportionality to the time constant obtained from Fig. 7 compared with the known thermal conductivity. The \mathcal{E}/T curve is normalized at 138 K.

particle-conservation equation (6), in the outer region. The theory also assumes that the plasma in the inner hot region is produced by thermal ionization, hence the term “magnetothermal pinch.”¹ By perturbing the two fundamental equations from their quasiequilibrium states, a dispersion relation is obtained which predicts

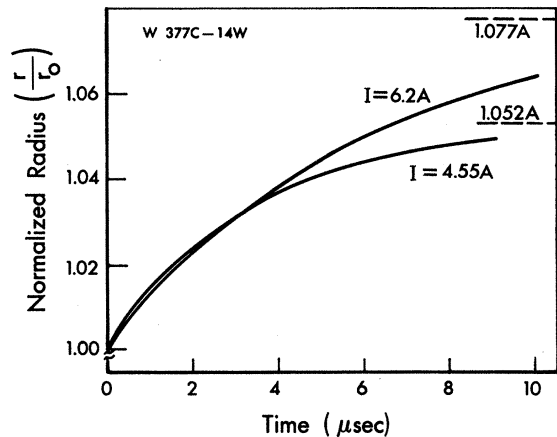


FIG. 9. Radius of the inner pinch region, normalized to the radius at $t=0$, as a function of time at two current levels showing the pinch expansion. The steady-state magnitudes are given by the dashed lines on the left-hand side.

oscillations in the electric field strength provided certain conditions are satisfied [Eqs. (22) and (23)]. When the experimental dependencies of the frequency on current and time are employed, the theoretically determined inner current and outer temperature are obtained. These values of I_i and T_0 are essentially uniquely defined and are consistent with the observed dependence of amplitude on current and time. These results are consistent with the known thermal conductance of InSb. Also, the pinch radius expands somewhat as time progresses, in agreement with the DAJ¹⁵ predictions about a slightly hollow pinch.

The theory has the following limitations. First, the actual dependence of mobility on temperature is more complicated than assumed. The $T^{-3/2}$ law used in this theory to describe the mobility is an approximation only applicable in the high-temperature range.¹⁹ Thus, this theory cannot be compared to the experimental results observed for ambients < 77 K, as described in Paper II. Second, it is certainly not true that two

temperature regions separated by a sharp boundary exist in the pinch. This condition is probably quite valid at early times when the hot channel is initially formed, but surely the boundary between the regions is diffuse at later times. Third, recombination is not negligible, as implicitly assumed in this theory, because the plasma density in the pinch is very high.

Although the magnetothermal pinch theory invokes several simplifying assumptions, it agrees well with the observed properties of the pinch oscillations. The several consistency checks plus the observed extent of agreement convince us that basically the theory is correct.

ACKNOWLEDGMENTS

The authors wish to express their gratitude to Dr. J. E. Drummond for his stimulating suggestions, particularly concerning the two-region pinch model, and to Dr. D. J. Nelson for his help in computer programming.

* Work done in partial fulfillment of the requirements for the PhD degree at the University of Washington.

† Research in the Department of Electrical Engineering partially supported by the National Science Foundation.

¹ B. Ancker-Johnson, in *Semiconductors and Semimetals*, 1, edited by R. K. Willardson and A. C. Beer (Academic, New York, 1966), p. 433.

² M. Glicksman and M. C. Steele, *Phys. Rev. Letters* **2**, 461 (1959).

³ B. Ancker-Johnson, R. W. Cohen, and M. Glicksman, *Phys. Rev.* **124**, 1795 (1961).

⁴ A. G. Chynoweth and A. A. Murray, *Phys. Rev.* **123**, 515 (1961).

⁵ B. D. Osipov and A. N. Khvoshchev, *Zh. Eksperim. i Teor. Fiz.* **43**, 1179 (1962) [*Soviet Phys. JETP* **16**, 833 (1963)].

⁶ M. Glicksman and R. A. Powlus, *Phys. Rev.* **121**, 1659 (1961).

⁷ B. Ancker-Johnson, in *Proceedings of the International Conference on Physics of Semiconductors, Exeter* (The Institute of Physics and the Physical Society, London, 1962), p. 141.

⁸ M. Toda, *Japan. J. Appl. Phys.* **2**, 467 (1963).

⁹ B. Ancker-Johnson, *Phys. Rev. Letters* **9**, 485 (1962).

¹⁰ M. Glicksman, *Japan. J. Appl. Phys.* **3**, 354 (1964).

¹¹ Y. Marechal, *J. Phys. Chem. Solids* **25**, 401 (1964).

¹² H. Schmidt, *Phys. Rev.* **149**, 564 (1966).

¹³ B. V. Paranjape, *J. Phys. Soc. Japan* **22**, 144 (1967).

¹⁴ Yu. L. Igitkhanov, *Zh. Eksperim. i Teor. Fiz.* **56**, 1619 (1969) [*Soviet Phys. JETP* **29**, 867 (1969)].

¹⁵ J. E. Drummond and B. Ancker-Johnson, in *Proceedings of the Seventh International Conference on the Physics of Semi-*

conductors 2: Plasma Effects in Solids (Academic, New York 1965), p. 173.

¹⁶ B. Ancker-Johnson and J. E. Drummond, *Phys. Rev.* **131**, 1961 (1963); **132**, 2372 (1963).

¹⁷ N. H. Nachtrieb and N. Clement, *J. Phys. Chem.* **62**, 876 (1958).

¹⁸ G. Busch and E. Steigmeir, *Helv. Phys. Acta.* **34**, 1 (1961).

¹⁹ C. Hilsun and A. C. Rose-Innes, *Semiconducting III-V Compounds* (Pergamon, New York, 1961), p. 126.

²⁰ From the ambipolar diffusion coefficient

$$D_A = \frac{[(n_0 + n)\mu_e D_h + (p_0 + n)\mu_h D_e]}{[(n_0 + n)\mu_e + (p_0 + n)\mu_h]} \approx (2\mu_e \mu_h) (\mu_e + \mu_h)^{-1} (kT/e),$$

the ambipolar mobility can be defined as

$$\mu_A = (2\mu_e \mu_h) (\mu_e + \mu_h)^{-1} \approx 2\mu_e m / M.$$

²¹ In Ref. 19, $\mu_e = 7 \times 10^4 T^{-1.6}$ m²/V sec. If the $T^{-1.5}$ law is substituted, μ_e may be transformed to $7 \times 10^4 \times (T_0^{1.5}/T_0^{1.6}) T^{-1.5} \approx 3.7 \times 10^4 T^{-1.5}$ m²/V sec, where T_0 is chosen to be 300 K.

²² K. F. Hulme and J. B. Mullin, *Solid State Electron.* **5**, 211 (1962).

²³ N. Mokrovskii and A. Regel, *Zh. Tekhn. Fiz.* **22**, 1281 (1952).

²⁴ P. V. Gul'tyaev and A. V. Petrov, *Fiz. Tverd. Tela* **1**, 368 (1959) [*Soviet Phys. Solid State* **1**, 330 (1959)].

²⁵ E. Burstein, G. S. Picus, and H. A. Gebbie, *Phys. Rev.* **103**, 825 (1956), for $m = 0.015m_0$; A. Mooradian and H. Y. Fan, *ibid.* **148**, 873 (1966), for $M = 0.45m_0$.

²⁶ H. S. Carslow and J. C. Jaeger, *Conduction of Heat in Solids*, 2nd ed. (Oxford U. P., Oxford, 1959), p. 93.